Proc. Int. Symp. Biomol. Struct. Interactions, Suppl. J. Biosci.,
Vol. 8. Nos 1 & 2, August 1985. pp. 121–139. © Printed in India.

Kringle 4 from human plasminogen: ^{1}H-nuclear magnetic resonance study of the interactions between ω-amino acid ligands and aromatic residues at the lysine-binding site

M. LLINÁS, A. MOTTA, A. DE MARCO* and R. A. LAURSEN**

Department of Chemistry, Carnegie-Mellon University, Pittsburgh, Pennsylvania 15213. USA

**Department of Chemistry, Boston University, Boston, Massachusetts 02215, USA

Abstract. The interactions of the ω-amino acid ligands ε-aminocaproic acid and *p*-benzylaminesulphonic acid with the isolated kringle 4 domain from human plasminogen have been investigated by ^{1}H-nuclear magnetic resonance spectroscopy at 300 and 600 MHz. Overall, the data indicate that binding either ligand does not cause the kringle to undergo significant conformational changes. When *p*-benzylaminesulphonic acid is in excess relative to the kringles, progressive exchange-broadening and high field chemical shifts are observed for the proton resonances of the ligand. The largest effect is seen at the amino end of the molecule, which indicates that the $-NH_3^+$ group of the ligand penetrates deeper into the binding site than does the $-SO_3^-$. Ligand-binding causes signals from the ring-current shifted Leu^{46} $CH_3^{\delta,\delta}$ groups and from a number of aromatic side-chains to shift. Depending on the ligand, the latter include Tyr-II (Tyr^{50}), Tyr-V (an immobile ring), His-II and His-III imidazole groups and the three Trp indole groups present in kringle 4. In particular, *p*-benzylaminesulphonic acid-binding induces large high field shifts on the Trp-II H6 triplet and the Trp-III (Trp^{72}) H2 singlet. On the other hand, ε-aminocaproic acid bound to kringle 4 exhibits large chemical shifts of its CH_2 proton resonances, which indicates that the lysine-binding site is rich in aromatic side chains.

Overhauser experiments centered on the *p*-benzylaminesulphonic acid H2,6 and H3,5 aromatic transitions as well as on the shifted Trp-II and Trp-III signals reveal efficient cross-relaxation between these two indole side chains and the *p*-benzylaminesulphonic acid ring. These experiments also show that the side chains from Phe^{64}, Tyr-II (Tyr^{50}), Tyr-IV, and His-II (His^{31}) interact with the ligand. In combination with reported chemical modification experiments that show requirement of Asp^{57}, Arg^{71} and Trp^{72} integrity for ligand-binding, our study underscores the relevance of the Cys^{51}-Cys^{75} loop in defining the kringles' lysine-binding site. Furthermore, the Cys^{22} -Cys^{63} loop is folded so as to place His^{31}, His^{33}, Tyr^{41} and Leu^{46} in proximity to the binding site. The involvement of residues within the Cys^{51}-Cys^{75} loop in ligand-binding suggests that Trp-II and Tyr-IV may correspond to Trp^{62} and Tyr^{74}, respectively. As shown by Overhauser experiments, these two residues are in close contact with each other. From these studies and from the shielding and deshielding effects caused by *p*-benzylaminesulphonic acid, we suggest that the ligand is sandwiched between the indole rings of Trp-II and Trp-III, which form part of the hydrophobic binding site.

keywords. Kringle 4; kringle structure; lysine-binding site; nuclear magnetic resonance; plasminogen.

Introduction

The heavy chain of plasmin, the active form of plasminogen, is structured by five homologous domains of molecular weight (M_r) ~ 10,000 each, known as kringles

---

*Permanent Address: lstituto di Chimica delle Macromolecole, Consiglio Nazionale delle Ricerche. Via E. Bassini 15/ A. 201 33 Milano ITALY

aminomethyl (cyclohexane)carboxylic acid; BASA. *p*-benzylaminesulphonic acid; K4, kringle 4; NOE, nuclear Overhauser effect; ppm, parts-per-million; pH*, glass electrode pH reading unconnected for deuterium isotope effects; rf, radio frequency; TSP. sodium 3-trimethylsilyl(2,2,3,3-$^2H_4$) propionate.

(Sottrup-Jensen *et al.,* 1978). It is well established that some of the plasmin(ogen) kringles, in particular kringles 1 and 4, are able to bind lysine and analogous ω-amino acids (Sottrup-Jensen *et al.,* 1978; Lerch *et al.,* 1980; Winn *et al.,* 1980; De Marco *et al.,* 1982), many of which exhibit potent antifibrinolytic properties (Okamoto *et al.,* 1968; Markwardt, 1978). All these ligands are dipoles-with an optimal charge separation of about 6·8 Å (Okamoto *et al.,* 1968; Winn *et al.,* 1980). Homologous kringles have been found in other proteins, several of which are thought to interact with fibrin(ogen) and, since they preserve the typical kringle structural outline (figure 1), it has been suggested that kringles might be considered as stereotypes of, or conserved modules carried by, protein-binding proteins (Patthy *et al.,* 1984). Therefore, the study of ω-amino acid ligand-binding to kringles is of considerable interest not only because of the central role plasmin(ogen) plays in hemostasis and in clinical thrombolysis, but also because it contributes to the better understanding of fundamental aspects of protein-protein interactions.

Up to now, a main effort has been directed to identifying the kringles' anionic and cationic centers that interact with complementary polar groups in the ligands. Thus, while Lerch and Rickli (1980) have suggested on the basis of chemical modification of kringles 1 and 4 and homology arguments that Asp^{55} and His^{31} (figure 1) might be involved in lysine-binding, Patthy and co-workers (Trexler *et al.,* 1982), have provided

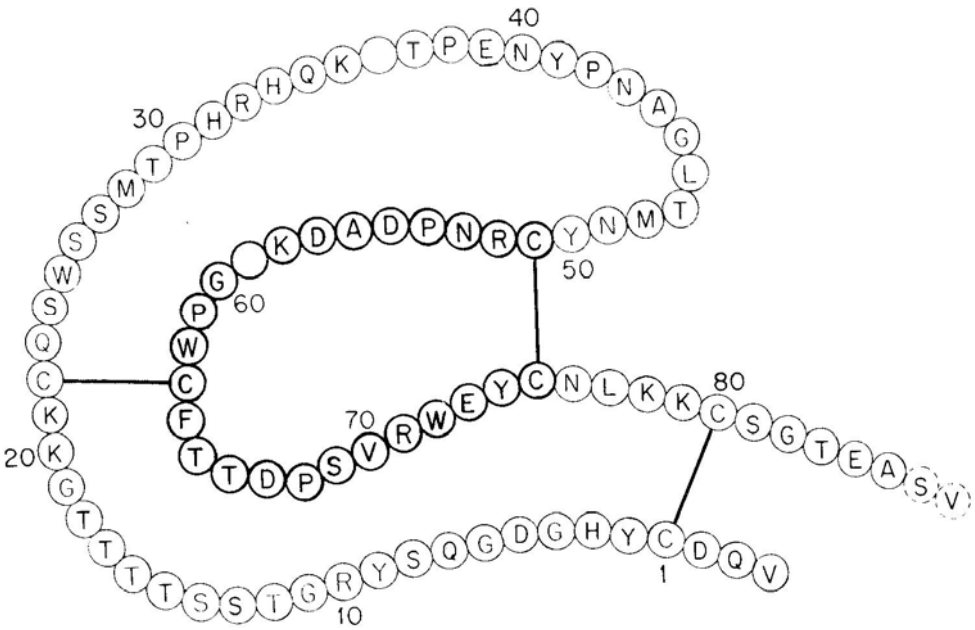

Figure 1. Primary structure of the K4 fragment from human plasminogen (Sottrup-Jensen *et al.,* 1978; Lerch *et al.,* 1980). Residues are numbered starting from the first half-cystine and the conventional one-letter code has been used to label the amino acid residues. K4 consists of residues – 2 to 85, but a second form, extending to residue 87, can be present in small amounts (Hochschwender *et al.,* 1983). Two deletions at sites 36 and 59 have been introduced to facilitate comparison with other kringles. Residues within the Cys^{51} –Cys^{75} loop, postulated to be involved in ligand-binding. are marked a heavy trace

chemical evidence that Asp^{57} and Arg^{71} (figure 1) are the most likely candidates in K4 for carrying the polar groups that balance the ligand electrostatic charges. There is also good evidence that Trp^{72} in K4 (Hochschwender and Laursen, 1981; Hochschwender *et al.,* 1983) and its replacement, Tyr^{72} in kringle 1 (De Marco *et al.,* 1982), are near the entry to the site. It was originally proposed (Winn *et al.,* 1980) and later substantiated by ^{1}H-nuclear magnetic resonance (NMR) spectroscopic evidence (De Marco *et al.,* 1982; Hochschwender *et al.,* 1983; Llinás *et al.,* 1983), that other interactions with hydrophobic, mostly aromatic, residues stabilize retention of the ligand at the binding site. In this paper we describe ^{1}H-NMR experiments aimed at uncovering those interactions and at better identifying amino acid residues at the lysine-binding site. Among the ligands that bind kringle 4 (K4), *p*-benzylaminesulphonic acid (BASA) and ε-aminocaproic acid (*ε*ACA) have been investigated. Both show potent antifibrinolytic activities (Okamoto *et al.,* 1968), and while the two ω-amino acids match the optimal dipolar distance of ~ 6·8 Å, they have different molecular structures: BASA contains a rigid aromatic ring, whereas εACA is composed of a flexible linear aliphatic chain. Thus, the two ligands are likely to afford valuable complementary information in a search for a general mechanism of ligand-binding. While this study was in progress, Trexler *et al.* (1983) published a paper which includes observations on the effect of *ε*ACA on the K4 spectrum.

Materials and methods

K4 was isolated by elastase digestion of human plasminogen as already reported (Sottrup-Jensen *et al.,* 1978; Winn *et al.,* 1980). *ε*ACA was purchased from Sigma and BASA belonged to a batch described by Hochschwender *et al.* (1983). Protein solutions for NMR studies were ~ 10^{-3} *M* in ^2H_2O. Proton-NMR spectra were recorded in the Fourier mode at 300 MHz on a Bruker WM-300 spectrometer and at 600 MHz using the NMR Facility for Biomedical Studies at Carnegie-Mellon University. Resolution enhancement, whenever implemented, was achieved by Gaussian convolution (Ernst, 1966; Ferrige and Lindon, 1978). Chemical shifts were determined from an internal dioxane signal and are referred to the sodium 3-trimethylsilyl-[2,2,3,3,-$^2H_4$]-propionate peak, assumed to be at – 3·766 ppm from dioxane (De Marco, 1977). Transient Overhauser experiments were run by selectively irradiating a transition between scans and allowing relaxation for 0·25 s before sampling. Many cycles of 8 scans off- minus on-resonance spectra were acquired in order to achieve a satisfactory signal-to-noise ratio. Nuclear Overhauser effect (NOE) spectra are shown as difference (unperturbed-minus-perturbed) spectra.

Results

The K4 spectrum shows two high field doublets at ~ 0·3 and ~ –1 ppm, stemming from the $CH_3^{\delta,\,\delta'}$ groups of Leu_{46} (figure 2A). Their appearance at these positions, also observed for kringle 1, has been justified by proposing ring-current effects stemming from a cluster of aromatic residues that interact with the Leu^{46} side chain (De Marco *et al.,* 1982; Llinás *et al.,* 1983). Indeed, Overhauser experiments from the signal at –1 ppm have identified rings from Trp-I, Trp-II, Tyr-III, and His-III as being in

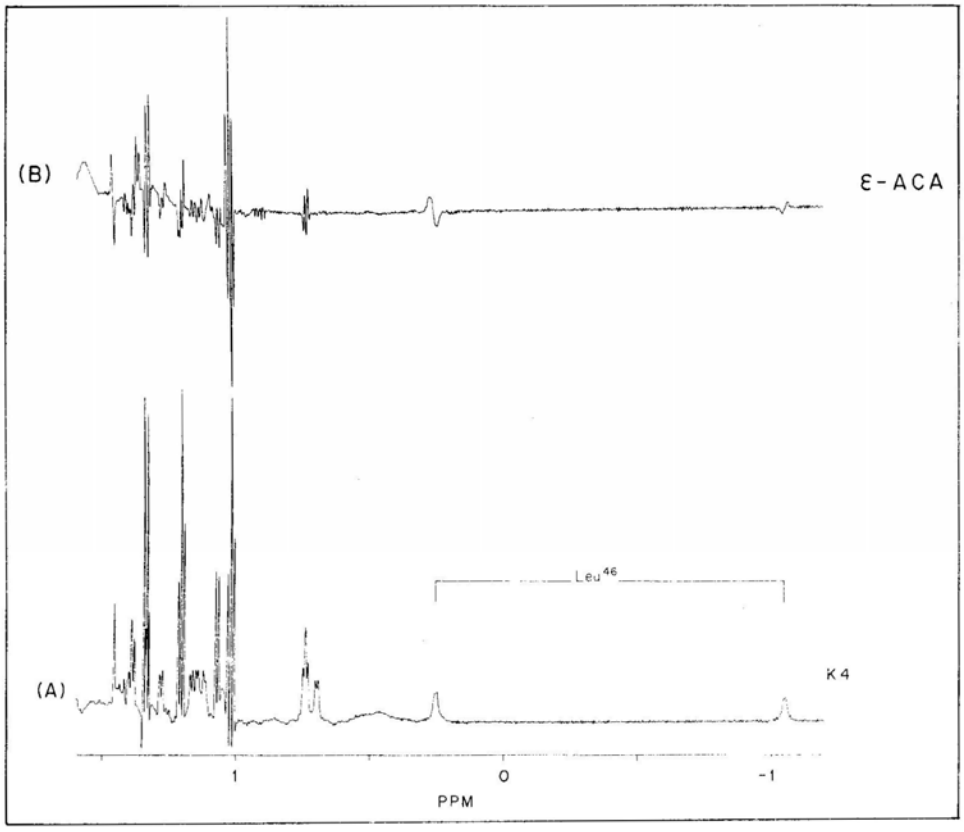

Figure 2. Effects of *ε*ACA-binding on the K4 methyl groups: ^{1}H-NMR spectra at 600 MHz. (A) Free K.4; (B) difference spectrum: spectrum of K4 + *ε*ACA (~ 1:11) minus spectrum A. The two ring-current shifted Leu$_{46}$ $CH_3^{\delta,\ \delta'}$ resonances are labelled in (A). K4 concentration ~ 10^{-3} *M*. pH* 7·2. 25°C. The spectra are resolution-enhanced.

efficient dipolar contact with the Leu^{46} methyl groups (Llinás *et al.,* 1983; Trexler *et al.,* 1983; De Marco *et al.,* 1985a). Because of their isolated positions, these doublets afford convenient probes for detecting the effects of ligands, as shifts have been observed for these resonances when BASA binds to kringle 1 (De Marco *et al.,* 1982) and to K4 (Llinás *et al.,* 1983). However, because BASA itself is an aromatic ligand, the shifts could arise either from conformational rearrangements of amino acid rings with which Leu^{46} interacts or from direct ring-current effects from the ligand. Hence, it is convenient to compare the perturbations caused by BASA with those resulting from aliphatic ligands. The effects stemming from *ε*ACA binding on the high-field methyl resonances are shown in figure 2B. Many sharp methyl lines between 0·5 and 1·5 ppm undergo small displacements (< 0·016 ppm) while the $CH_3^{\delta,\ \delta'}$ doublets of Leu^{46} experience somewhat more pronounced shifts (~ 0·032 ppm). As shown, the Leu^{46} signal at 0·3 ppm shifts more than the one at –1 ppm. Similar effects are observed when AcLys and AMCHA

are the ligands (to be published), while in the case of BASA it is the signal at – 1 ppm that shifts the most (Llinás *et al*., 1983). In a preliminary folding model of K4, which qualitatively accounts for the dipolar connectivities established by Overhauser experiments (De Marco *et al.,* 1985a), Leu[46] is centered in a hydrophobic core contiguous to the ligand-binding site. Hence, the perturbation of the Leu[46] spectrum by both BASA and aliphatic ligands should be interpreted as resulting from local conformational rearrangements of aromatic rings within the hydrophobic core which, in turn, induce the spectral changes through ring-current shifts.

Figure 3A shows expanded the spectral region between the two methyl resonances of Leu[46]. Upon a first addition of *ε*ACA, five resonances, labelled a-e, appear proximal to the two Leu[46] methyl signals (figure 3B). By increasing the *ε*ACA/K4 ratio they shift toward low-field and disappear when saturation is reached (figure 3C-E) to emerge at the free ligand position. At sub-stoichiometric ligand levels, the amplitude of these

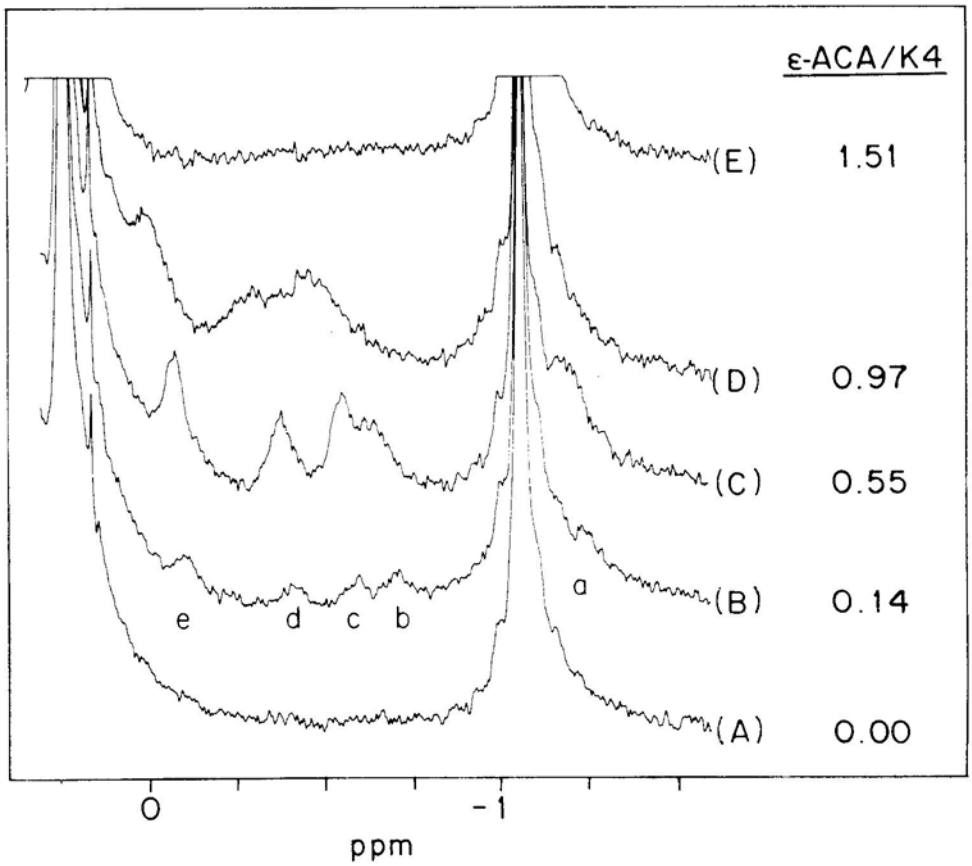

Figure 3. *ε*ACA bound to K4: shifted resonances at 600 MHz. Five resonances stemming from the CH_2 groups of the ligand are labelled a-e. As the ratio *ε*ACA/K4 increases toward saturation, the resonances move toward the free ligand positions (B-E). Kringle concentration ~ 10^{-3} *M*; pH* 7·2, 25°C.

resonances increases with ligand concentration, indicating that they stem from the CH_2 groups of bound *ε*ACA. The ligand signals appear severely shifted from their standard positions ($\delta \gtrsim 0{\cdot}8$ ppm), most likely a reflection of anisotropic ring-current effects comparable to those experienced by the Leu^{46} $CH_3^{\delta,\delta'}$, doublets. Similar effects are observed when N^{α}-acetyl-L-lysine is the ligand (to be published). We interpret the upfield shift experienced by the bound ligand CH_2 resonances (figure 3) as strong indication of a direct interaction between the ligand and the face of aromatic side chain(s) at the binding site.

The aromatic ^{1}H–NMR spectrum of K4 has been studied in detail and the spin systems of individual residues identified (De Marco *et al.,* 1985b). Figure 4 illustrates the effects of *ε*ACA on the aromatic resonances of K4, where the main shifts induced by ligand-binding are indicated by broken vertical lines connecting spectra A and B. [The addition of ligand brings about a slowing of the ^{1}H-^{2}H exchange kinetics, as indicated by the presence of residual amide NH resonances in spectrum B (De Marco *et al.,* 1985c)]. Two Trp-I (Trp^{25} or Trp^{62}) indole one-proton resonances, a H5 triplet at

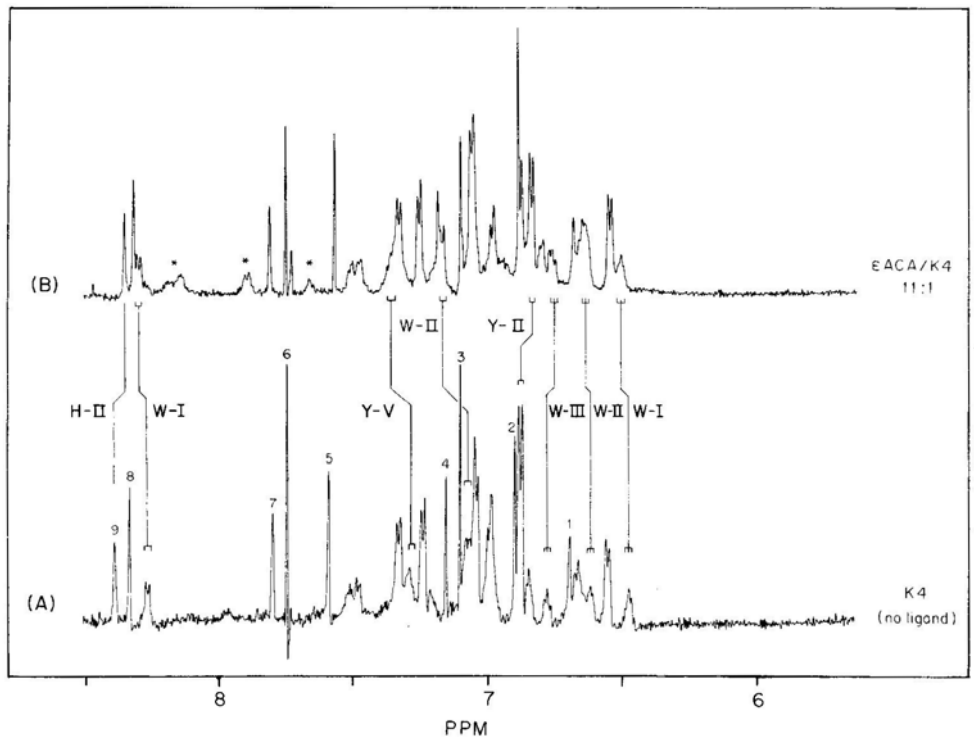

Figure 4. Effect of *ε*ACA-binding on the K4 aromatic side chains: ^{1}H-NMR spectra at 600 MHz. (A) Free K4; (B) K4/εACA ~ 1:11. Resonances discussed in the text are connected by broken vertical lines, denoting shifts originating from the presence of ligand. The conventional one-letter code is used to label resonances according to amino acid origin. His and Trp singlets are numbered 1–9. Some minor signals originating from partially exchanged amide NH groups in spectrum (B) are indicated by an asterisk (*). The K4 concentration was 10^{-3} *M*, pH* 7·2, 25° C. Both spectra are resolution-enhanced.

~ 6·5 ppm and a H4 doublet at ~ 8·3 ppm, are clearly affected by the ligand. Interestingly, the Trp-II (Trp^{62} or Trp^{25}) triplet at ~ 6·6 ppm (H6) and doublet at ~ 7·1 ppm (H7) and the Trp-III (Trp^{72}) triplet at 6·8 ppm (H5 or H6), also undergo shifts, supporting the proposed interactions among the three Trp indoles present in K4 (Llinás *et al.,* 1983). Also affected are the His-II (His^{31}) H4 resonance at ~ 8·4 ppm (singlet 9) and a Tyr doublet at ~ 6·9 ppm, originating from either Tyr-II or Tyr-IV which overlap at this position. Most informative, is the shift of a one-proton Tyr-V resonance at ~ 7·3 ppm, whose phenol group is buried as it is immobile on the 600 MHz spectrometer time-scale (De Marco *et al.,* 1985b). All these residues are perturbed by the ligand and, therefore, are likely to be part of, or lie in the immediate proximity to, the lysine-binding site.

The 300 MHz ^{1}H-NMR spectrum of the ligand BASA in $^{2}H_2O$ solution is shown in figure 5B, which shows expanded (inset) the aromatic multiplets arising from protons

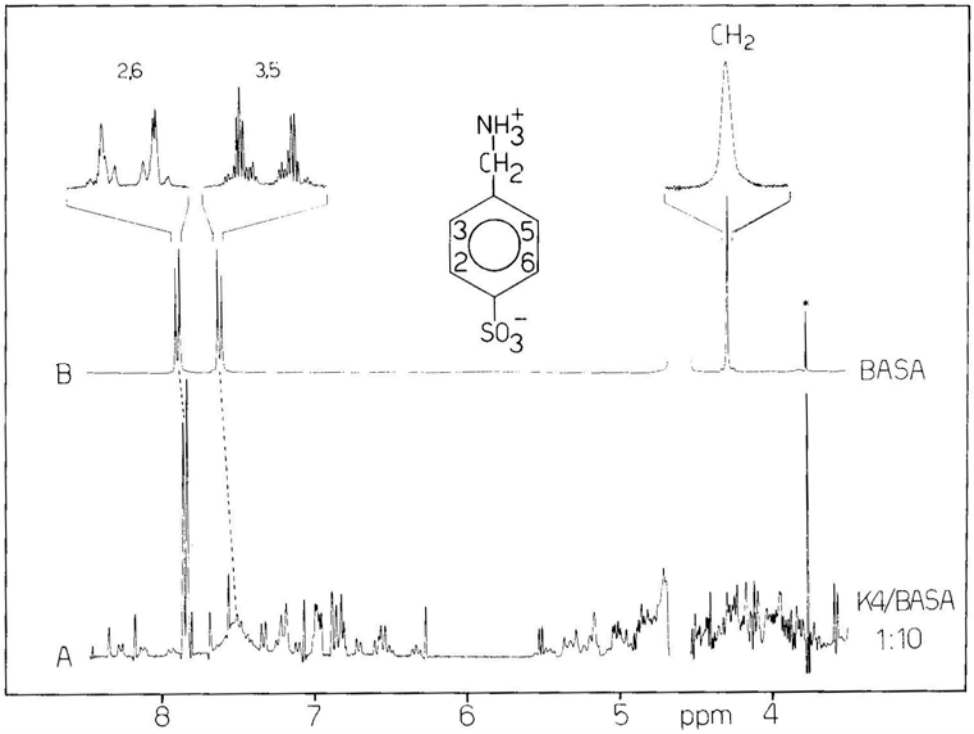

Figure 5. Effect of kringle-binding on the BASA ligand: ^{1}H-NMR spectra at 300 MHz. (A) K4/BASA ~ 1:10; (B) free BASA. Dashed lines connect corresponding BASA signals in spectra A and B, indicating high field shifts for identified resonances of bound ligand. The kringle concentration was ~ 10^{-3} *M*, pH* 7·2, 45°C. The strong $^{1}H^{2}HO$ signal has been omitted in spectra A and B, which are shown resolution-enhanced. In B, an asterisk (*) indicates the dioxane resonance, used as internal reference standard. The insert shows an expansion of the BASA aromatic and methylene signals after strong resolution enhancement and Fourier transform over 64K data memory. The BASA resonances have been assigned from their multiplet fine structure and *via* Overhauser experiments.

ortho (H2, H6, ~ 7·95 ppm) and *meta* (H3, H5, ~ 7·70 ppm) to the anionic group and the somewhat broad, structureless resonance from the methylamino methylene group at ~ 4·30 ppm. In the presence of 1/10 its concentration of K4, the free ligand resonances experience a shift and gain in breadth. As illustrated in figure 5A, the BASA CH_2 resonance is broadened beyond detection while the aromatic H2,6 multiplet remains comparatively sharp and shifts by ~ – 0·08 ppm. Intermediate between the extremes exemplified by these two signals is the broadening experienced by the aromatic H2,6 multiplet which shifts ~ – 0·16 ppm. The observed effects can be summarized by stating that they increase on going from the ring H2,6 to the CH_2. The broadening suggests that the BASA methylamine group and, to a lesser extent, the aromatic ring, sense two very different environments while the ligand fluctuates between its free and bound states. It is suggested (Llinás *et al.,* 1983) that the positively-charged end of the ligand is the one that penetrates deeper into the lysine-binding site, presumably to pair itself with an anionic center (Asp^{57}), while the negative end of the ligand, which most likely interacts with a cationic center (Arg^{71}) (Trexler *et al.,* 1982), is more exposed to the solvent, as indicated by the relative sharpness of the ortho resonance (figure 5A). Furthermore, the high field shifts observed for both BASA and the aliphatic ligands indicate that the lysine-binding site is predominantly structured by aromatic residues which in turn cause the ring-current effects on the ligand resonances.

The effects of BASA on the aromatic resonances of K4 are reported in figure 6A.B. In this case a lower ligand/K4 ratio was used in order to obtain a kringle spectrum unobscured by aromatic BASA signals. We notice that most signals perturbed by εACA are also sensitive to BASA, although for some resonances the induced shifts are amplified in the case of the aromatic ligand. This is most conspicuous for singlet 4 (Trp-I H2) which is barely affected by εACA (figure 4). A number of Trp-I resonances (H5 triplet at ~ 6·5 ppm, H2 singlet at ~ 7·2 ppm, and the H4 doublet at ~ 8·3 ppm, figure 6A) shift to low fields, in analogy to their response when εACA is the ligand (figure 4B). A magnetic deshielding is also observed for the one-proton doublet of Tyr-V at 7·3 ppm. These responses suggest that Trp-I and Tyr-V are somewhat removed from the ligand so that they experience only small effects caused either by the anisotropic shielding of the BASA ring or by conformational rearrangements induced by the ligand. The latter seems more likely considering that, as described below, no NOEs are observed on the above residues when BASA is irradiated. High-field shifts are experienced by singlet 8 (His-III H2) when in the presence of BASA (figure 6B) and singlet 9 (His-II H4) when in the presence of εACA (figure 4B), but they are essentially unperturbed when the presence of the other ligand, εACA and BASA, respectively. It has been found that AMCHA affects the latter two singlets in a way similar to BASA (to be published). In AMCHA the phenyl group present in BASA is substituted with a cyclohexyl ring, thus retaining some of the ring rigidity while avoiding intrinsic ring current effects. Thus, the His-III (His^{33}) sensitivity to ligand-binding is likely to result from local conformational rearrangements required to accommodate the more rigid cyclic ligands. Interestingly, the high field shift of the Tyr-II doublet observed in the presence of εACA (figure 4B) is smaller when BASA is the ligand (figure 6B) [Tyr-IV, which overlaps with Tyr-II at 6·9 ppm, is excluded by Overhauser experiments (figure 6A′, B′ since the Tyr-IV doublet at 6·9ppm in the ligand free K4 (figure 6A′) is recovered at the same positions in K4 in the presence of a two-fold molar excess of

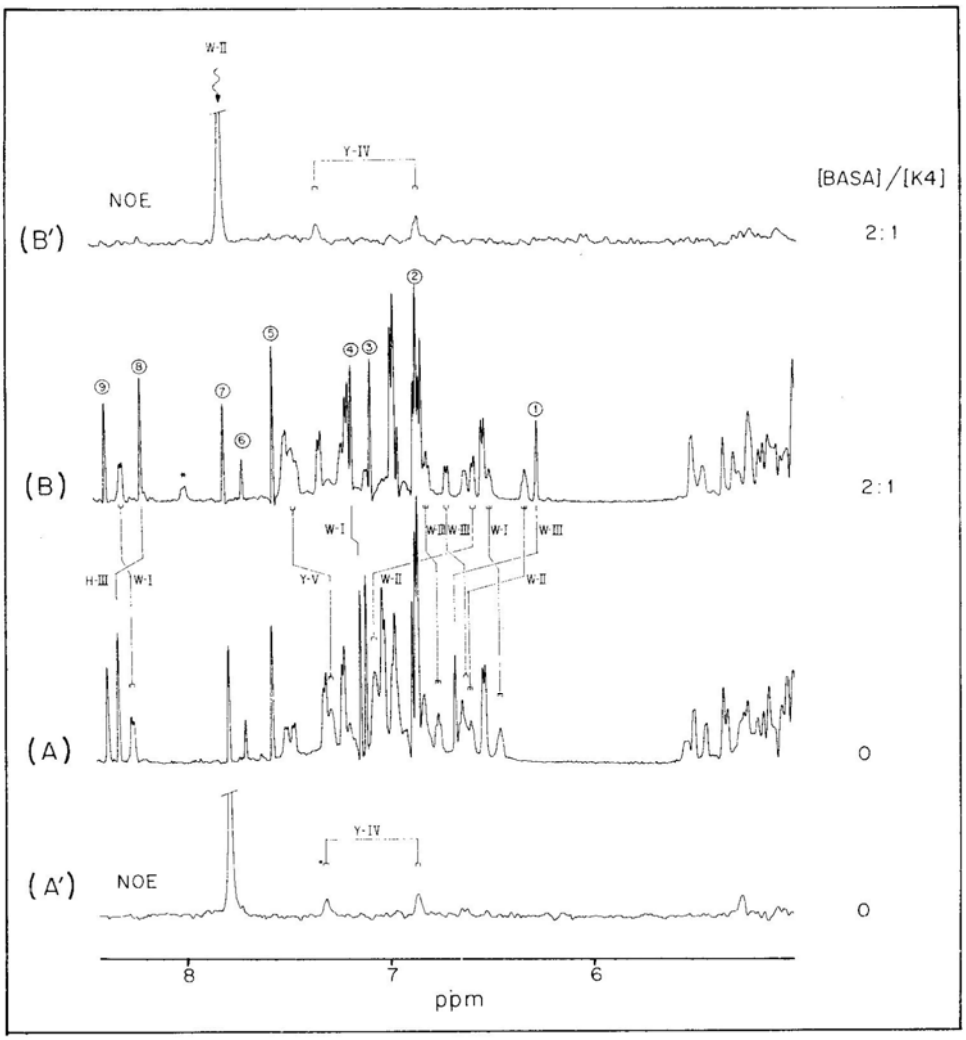

Figure 6. Effect of BASA on the K4 aromatic resonances: ^{1}H-NMR spectra at 600 MHz. (A) Reference spectrum, no ligand; (B) perturbed spectrum. 2:1 BASA/K4. Most marked chemical shifts induced by the ligand are indicated by broken vertical lines. The conventional one-letter code is used to label resonances according to amino-acid origin. His and Trp singlets are numbered 1–9 (Llinás *et al.*, 1983; De Marco *et al.,* 1985b). A and B are NOE difference spectra generated by irradiating the Trp-II indole H2 singlet for 25 ms, yielding ~ 70% inversion. for the kringle in presence (B')tand absence (A')tof BASA. K4 concentration 1 mM. pH* 7·2. 25°C; for the Overhauser experiments. 250 ms build-up wait period before sampling and 2·5 s recycling time

BASA (figure 6 B′)]. From figure 6B it is clear that Trp-II and Trp-III (Trp^{72}) undergo the largest high-field shins in the presence of BASA. suggesting that they are in direct contact with the ligand: In fact, hydrophobic interactions often place the protons above the center of the aromatic ring, *i.e.,* where the shielding is greatest (Perkins, 1982). In

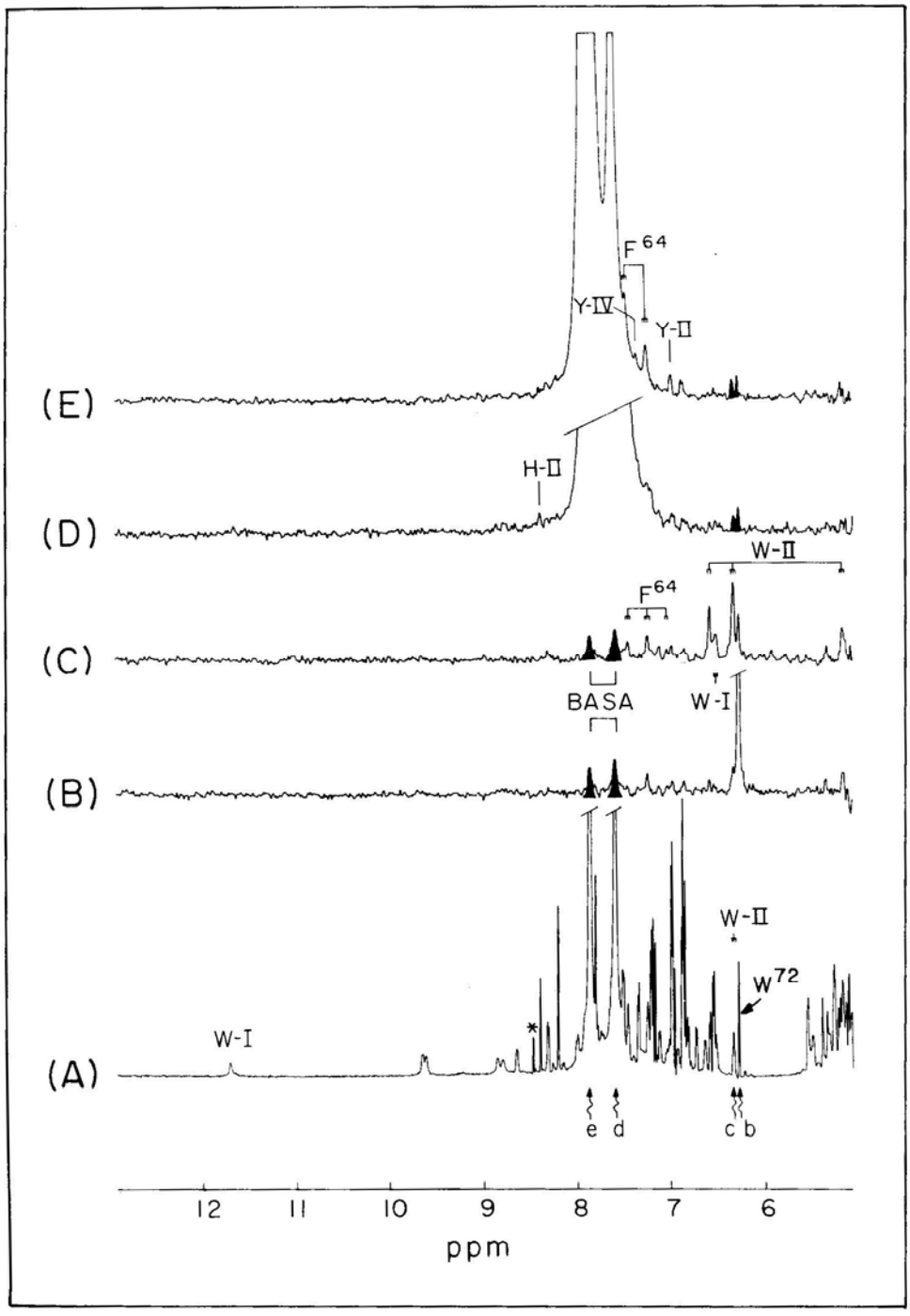

Figure 7. Ligand-K4 proton Overhauser experiments at 600 MHz: K4 in presence of ten-fold excess BASA. (A) Reference spectrum; (B), (C). (D)and (E) NOE difference spectra upon irradiation of Trp^{72} H2 singlet 1 (resonance b, spectrum A). Trp-II H6 triplet (resonance c.

contrast with the shifts of the Leu[46] $CH_3^{\delta,\delta'}$ doublets, which results from binding either aliphatic ligands or BASA, the latter Trp resonances are negligibly perturbed when in the presence of εACA, which suggests that the observed shifts might result from *direct* ligand ring-current effects on Trp indoles positioned at close distance rather than from conformational rearrangements of neighbour aromatic side chains. Therefore, the Trp-II and Trp-III indole rings might serve as convenient reporter groups with which to investigate the lysine-binding site by Overhauser experiments aimed at detecting BASA-kringle cross-relaxation.

Figure 7 shows the 600 MHz aromatic spectrum of K4 when it presence of 10:1 excess BASA (A) and its response to irradiation of the ring-current shifted Trp-III (Trp[72]) H2 singlet (B), the Trp-II H6 triplet (C), and the BASA aromatic transitions (D,E). The excited resonances are labelled b-e in the reference spectrum (A). The selectivity of each experiment was estimated by assuming a Gaussian power distribution for the rf pulse excitation and measuring the perturbation of the resonance closest to the irradiated one. For example, for the experiments depicted in figure 7B,C, perturbation of the triplet at 6·33 ppm is observed when irradiating the singlet at 6·27 ppm (figure 7B), and, for the experiments shown in figure 7D,E, the singlet at 7·80 ppm when irradiating the BASA peaks d and e (figure 7A). Irradiation of the Trp III (Trp[72]) indole H2 singlet at 6·27 ppm elicits definite responses, albeit of lesser amplitude, at 7·89, 7·59, 7·23 ppm and elsewhere, (figure 7B). The first two peaks are readily identified as BASA signals, while the third one originates from the two-proton H2,6 doublet of the Phe[64] ring (De Marco *et al.,* 1985b). NOEs of lesser amplitudes reveal proximity of Tyr-I and Tyr-II to Trp-III (Trp[72]) . Irradiation of the Trp-II indole H6 triplet at 6·33 ppm yields both intra-side chain NOEs, indicated in figure 7C by lines connecting a Trp-II doublet (6·57 ppm)+triplet (5·15 ppm) to the irradiated triplet (6·33 ppm), as well as strong effects on the H5 triplet of Trp-I (6·51 ppm) and on the BASA transitions at 7·89 and 7·59 ppm (blackened peaks, figure 7C). Interestingly, the complete set of Phe[64] resonances (De Marco *et al.,* 1985b) is recovered in the NOE spectrum (F^{64} stick diagram) as well as peaks previously observed when irradiating the singlet at 6·27 ppm (figure 7B). Irradiation of the H3,5 BASA signal at 7·59 ppm perturbs the signal from vicinal H2,6 ring protons but, more interestingly, it also affects the Trp-II triplet + Trp[72] singlet amplitudes at ~ 6·3 ppm (blackened peaks in figure 7D). This experiment also indicates some minor dipolar interactions with other aromatic groups that show up just above noise level in the NOE difference spectrum. It should be noticed that, because of crowding of resonances between 7·5 and 8·0 ppm, lower rf power was used in experiments D and E (compared with experiments B and C), which decreases the relative-intensities of the latter NOEs.

---

spectrum A), and BASA H2.5 and H3,6 aromatic transitions (resonances d and e, respectively, spectrum A). The irradiated transitions are indicated by wavy arrows in spectrum A. Individual side chain spin systems in the perturbed spectra are shown connected (stick diagrams), and labelled according to the conventional one-letter code. Soft pulses of 25 ms, yielding ~ 65% inversion, were used as excitations for resonances b and c; while for d and e low power irradiation applied for 50ms was implemented (~15° inversion). Each NOE difference spectrum averages 8000 scans off-resonance minus 8000 scans on-resonance, with 0·25 s build-up wait period before sampling and 2·5 s recycling time. Kringle concentration ~ 10^{-3} *M*, pH* 7·2. 25°C. Spectrum A is resolution enhanced.

His-II (His^{31}) is likely to be in close contact with other aromatic residues as indicated by its reversed spectral pattern, *i.e.*, with the H4 singlet resonating at lower field than the H2 singlet (Llinás *et al.,* 1983; De Marco *et al.,* 1985b). BASA-binding to K4 (figure 6A, B) indicates that His-II imidazole H2 and H4 resonances, singlets 5 and 9. respectively, are not significantly shifted by the ligand (Hochschwender *et al.,* 1983; Llinás *et al.,* 1983)and that neither is the corresponding imidazole NH3 (to be published). However, as shown in figure 7D, a definite NOE is observed on the His-II H4 singlet at ~ 8·4 ppm upon irradiation of the H3,5 (but not the H2, 6) BASA transition. The reverse experiment, in which the His-II H4 singlet was irradiated, confirms cross-relaxation between BASA and His-II (not shown). This, combined with the observation that the His-II H4 shifts with εACA (figure 4) and the detection of BASA H3,5-His-II cross-relaxation, indicates that the His-II (His^{31}) imidazole is close to the deeper, negatively charged, end of the lysine-binding site.

Upon irradiation of the BASA *ortho* H2,6 signal at 7·86 ppm (figure 7E) we recover, besides the signal from vicinal BASA *meta* H3,5, the Trp-III + II singlet + triplet at ~ 6·3 ppm (blackened peaks) as well as definite Phe^{64} and phenol (Tyr-II and/or Tyr-III, which overlap at 6·97 ppm, and Tyr-IV) NOEs. The fact that NOEs of negative sign are observed between the aromatic BASA signals indicates that the ligand bound to K4 behaves like a macromolecule of restricted mobility for which, the NOE is expected to be negative (Bothner-by. 1979).

Irradiation of resonances in a crowded spectral region are complicated by selectivity problems. Spillover effects were tested by running the same experiments as shown in figure 7 on a sample of kringle 4 in the presence of BASA with a ligand/kringle ratio of ~ 2, at which concentrations the spectral pattern of a fully complexed kringle is apparent while the aromatic BASA resonances are exchange-broadened beyond detectability (Hochschwender *et al.*, 1983). The experiments are depicted in figure 8 and the irradiated frequencies are indicated by arrows in the reference spectrum A, where d and e indicate the positions at which the aromatic BASA protons resonate when the ligand is in excess (figure 7A). NOEs stemming from irradiations of the singlet and triplet at 6·27 and 6·33 ppm are shown in figure 8B, C, respectively. It is apparent that BASA signals at 7·59 and 7·89 ppm do not show up in the difference spectra (B, C), while all other effects previously observed when in the presence of excess BASA, are recovered (figure 7B, C). Furthermore, irradiation at blank positions d and e, where the BASA signals appear (figure 7), generates rf power spillover effects but no detectable NOEs in the aromatic spectrum (figure 8D, E), which confers validity to the ligand-kringle NOEs shown in figure 7D and E.

Overhauser experiments were implemented (figure 6) in which the Trp-II H2 resonance (singlet 7 at ~ 7·8 ppm) was selectively inverted both in the absence (A′) and in the presence (B′) of BASA. In the two experiments, the only clear response was from the Tyr-IV phenol, which happens to be one of the NOEs detected in figure 7E, when BASA is irradiated. However, in figure 7E, the Tyr-IV NOE must be assumed to arise from the ligand-kringle cross-relaxation since in the corresponding control experiment (figure 8E) no such NOE is apparent. The experiments in figure 6A′, B′ unequivocally demonstrate that the Tyr-IV ring is positioned extremely close to the Trp-II indole H2, to the extent that it may play a major role in determining the low-field position of the H2 resonance. Furthermore, from figure 6, spectra A' and B'. it is apparent that the Tyr-

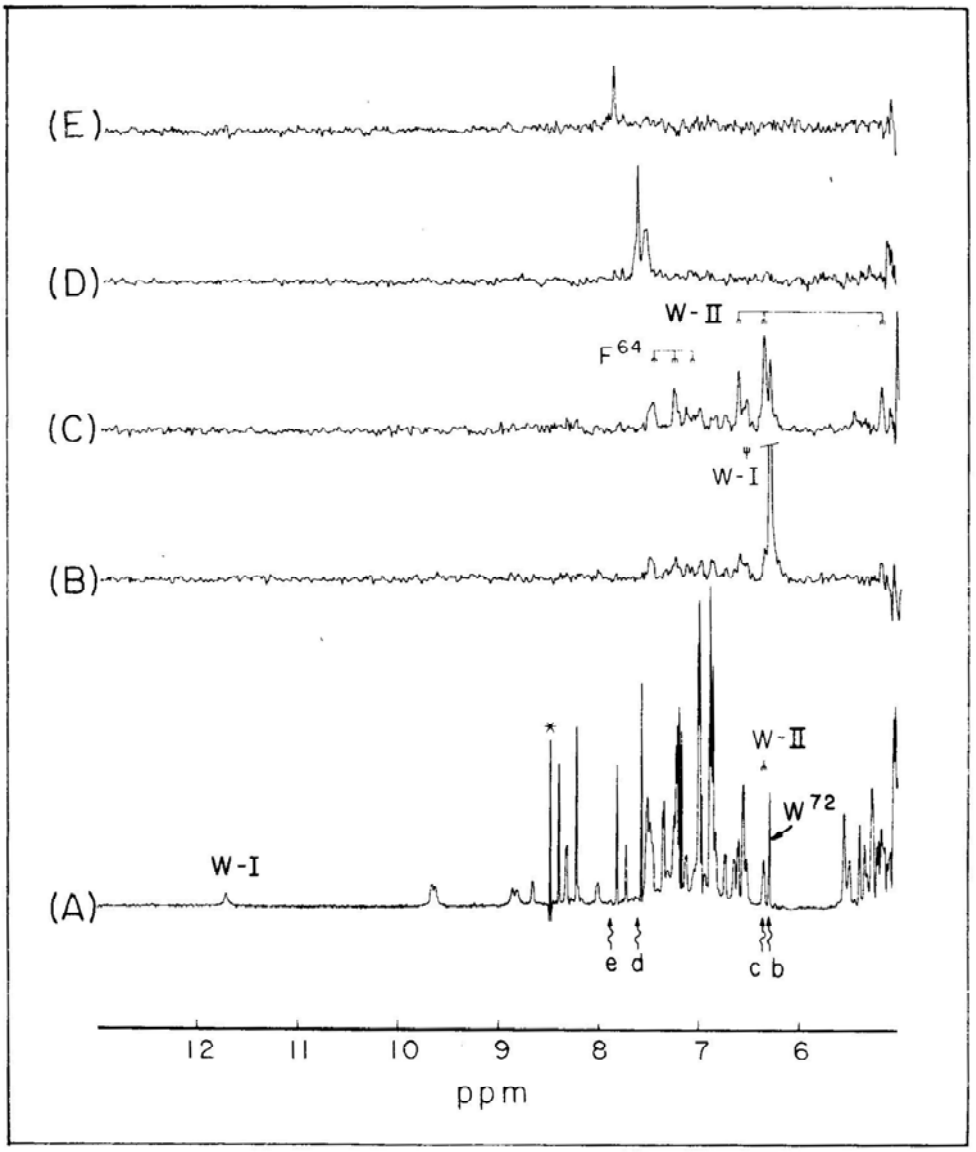

Figure 8. Control Overhauser experiments at 600 MHz: K4 in presence of 2:1 excess BASA. (A) Reference spectrum of the BASA/K4 complex; (B), (C), (D), and (E) difference spectra obtained by irradiating Trp^{72} H2 singlet 1 (resonance b, spectrum A), Trp-II H6 triplet (resonance c, spectrum A), and the frequencies at positions d and e (spectrum A) where the BASA resonances appear in figure 7A. The irradiated positions are indicated with wavy arrows in the reference spectrum A. Experimental conditions, including rf irradiation power are identical to those described in figure 7. Spectrum A is resolution-enhanced.

IV doublet at ~ 7·3 ppm is shifted by BASA and taking into account that a ligand-kringle NOE is detected on this same Tyr-IV signal (figure 7E) a model is suggested where the Tyr-IV ring should be placed in proximity to the lysine-binding site.

Discussion

Our study concurs with that of Trexier *et al.* (1983) concerning the effect of εACA on the K4 spectrum. Interestingly, despite their differing molecular structures, qualitatively similar perturbations are introduced in the K4 aromatic spectrum by BASA and by εACA. Table 1 lists the BASA-induced shifts measured on the K4 Trp aromatic resonances. It is evident that while BASA-binding causes all the Trp-I indole resonances to shift low-field to a similar extent, these are significantly less affected than those of the other two Trp side chains. The two indoles which exhibit the larger shifts are variously affected: The largest high-field shifts are observed for the Trp-II H6 and H7 multiplets and the Trp-III (Trp^{72}) H2 singlet while the Trp-II H1 and H5 resonances are the signals which shift the most to low fields. In a benzene ring, the ring-current effect generates two zones: one of shielding above and below the ring, and one of deshielding, maximal in the ring plane. Therefore, assuming that the shifts reported in table 1 originate from BASA only, we expect the H6 and H7 of Trp-II, and the H2 of Trp^{72} to be placed in the shielding zone of BASA. while the H1 and H5 of Trp-II would be in the corresponding deshielding zone. An attempt was made to estimate the distances between BASA and the side chains of Trp-II and Trp^{72}, by using the ring shielding

Table 1. BASA-induced shifts on the Trp indole resonances of K.4. Data are taken from spectra recorded at 330K, pH* 7·2 for solutions in ^2H_2O (De Marco *et al.,* 1985b) and at pH 7·6 for solutions in ^1H_2O (unpublished).

Tryptophan[a]	Proton	K4 (ppm)	2:1 BASA/K4 (ppm)	$\Delta\delta^b$ (ppm)
Trp-I	H1[c]	11.61	11.68	0.07
	H2	7.14	7.19	0.05
	H4	8.24	8.27	0.03
	H5	6.46	6.51	0.05
	H6	4.97	5.03	0.06
	H7	7.46	7.49	0.03
Trp-II	H1[c]	10.42	10.74	0.32
	H2	7.80	7.81	0.01
	H4	6.95	7.10	0.15
	H5	4.77	5.18	0.41
	H6	6.58	6.34	−0.24
	H7	7.10	6.61	−0.49
Trp-iII	H1	—	—	—
	H2	6.67	6.29	−0.38
	H4 or H7[e]	6.66	6.70	0.04
	H5 or H6[e]	5.10	5.18	0.08
	H6 or H5[e]	6.72	6.82	0.10
	H7 or H4[e]	7.05	7·20	0·15

[a]Trp-III has been assigned to Trp^{72} (Llinás *et al.,* 1983; Trexier *et al.,* 1983). Trp-I and Trp-II are likely to correspond to Trp^{25} and Trp^{62} (see text).

[b]Positive and negative numbers indicate low-field and high-field shifts, respectively.

[c]Value measured in ^1H_2O, pH 7.6.

[d]Resonance not yet identified.

[e]Ambiguous assignment (De Marco *et al.,* 1985b).

effects calculated for benzene by Bovey (1969). By assuming that the Trp-II and Trp-III shieldings and deshieldings originate exclusively from BASA, we obtained good agreement between experimental and the Bovey values only by stacking the indole groups ~ 1·5 Å from BASA, on each side of the ligand ring. Closest Van der Waals distances between two aromatic rings have been assumed to be ~ 3·5 Å (Perkins, 1982), which suggests either that the BASA ring-current effects are overestimated, so that other aromatic contributions should be taken into consideration, or that contacts closer than allowed by the Van der Waals radii contribute to the large Trp shifts.

Taking into account that for the Overhauser experiments in figure 7 the wait period after inversion of the irradiated resonance is relatively short (0·25 s), an efficient dipolar interaction is indicated between BASA and Trp^{72} (Trp-III), Trp-II, His^{31} (His-II), Tyr-II (and/or Tyr-III), Tyr-IV, and Phe^{64}. NOEs reported in this paper and elsewhere (De Marco *et al.,* 1985a) are summarized by the connectivities indicated in figure 9. The diagram provides insights into which residues might contribute to ligand-binding. It is interesting to notice the position of BASA with respect to the three Trp side chains: The connectivities require BASA to be in direct contact with, and centrally placed with regard to, the Trp-II and Trp-III (Trp^{72}) indoles. Indeed, the areas of the BASA. NOEs (difference spectra) upon irradiation of the shifted H6 triplet (Trp-II) and H2 singlet (Trp^{72}) are very similar (figure 7B, C). In contrast, Trp-I is likely to be somewhat removed from the binding site, as indicated by the absence of an NOE from the ligand. This is consistent with the relatively lesser sensitivity of the Trp-I indole chemical shift to ligand-binding, as described above. Indeed, the Trp-I NH resonance at ~ 11·8 ppm (figures 7,8) which is protected by BASA against solvent ^2H exchange (De Marco *et al.,* 1985c), is also insensitive to BASA irradiation (figures 7D, E) and does not significantly shift upon ligand-binding. Furthermore, upon irradiation of the Trp-II H6 triplet, both Trp-I and Trp-III (Trp^{72}) are recovered, while irradiation of the Trp^{72} H2 transition brings about effects on Trp-II but not on Trp-I. In the absence of ligand (De Marco *et al.,* 1985a) only Trp-II showed NOEs upon irradiation of Trp^{72} (Trp-III), while no response was obtained from Trp-I (figure 9). Conversely, when irradiating Trp-I strong perturbations were observed for Trp-II solely. On the basis of these observations, it is reasonable to imagine that Trp-II separates Trp-I from Trp-III (Trp^{72}) (figure 9) and, since irradiation of other transitions affected those resonances that are perturbed when the same transitions are excited in the presence of BASA, it is indicated that K4 does not significantly change its conformation upon ligand-binding.

The dipolar connectivity diagram in figure 9 accounts for the observations that both BASA (Llinás *et al.,* 1983) and *ε*ACA (figure 2) perturb the Leu^{46} spectrum indirectly, due to conformational rearrangements of aromatic residues interposed between the binding site and Leu^{46}. The connectivities also justify why Overhauser experiments centred on BASA or on the Leu^{46} $CH_3^{\delta,\delta'}$ resonances fail to reveal cross-relaxation between the two groups, while perturbing residues in their periphery (figure 9, heavy-traced circles around Leu^{46}). The diagram further suggests that BASA approaches the binding site from the left, establishing direct contact with Tyr-IV, Phe^{64}, Trp^{72} (Trp-III) and Trp-II, while the hydrophobic core, operationally defined as Leu^{46} and its surroundings, is contiguous to the site and probably contributes to its scaffolding.

The large shifts experienced by the CH_2 resonances from *ε*ACA bound to K4 (figure 3) suggest a direct interaction between the ligand and the face of aromatic side

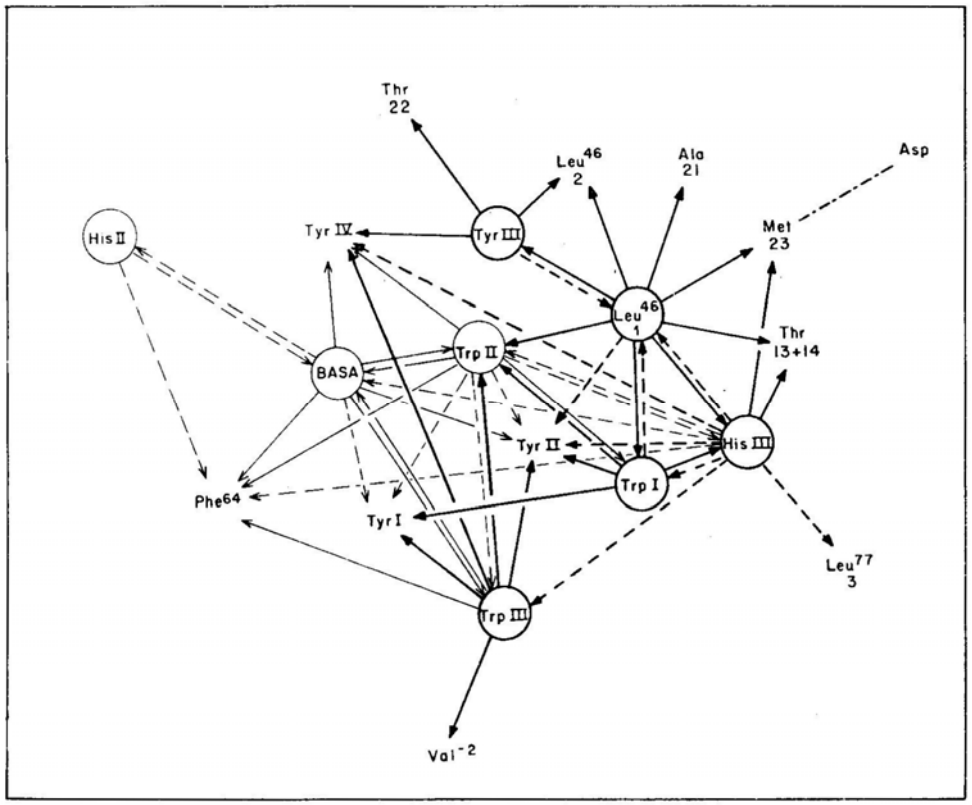

Figure 9. K4 ligand-binding site and hydrophobic core. The connectivities are all derived from Overhauser experiments (arrows) except for the one between Met CH_3^{ε} singlet and an Asp or Glu residue (–·–) established by acid/base titration. The heavy trace arrows and circles indicate NOE connectivities among residues at the hydrophobic cluster centered on Leu^{46} (De Marco *et al.*, 1985a). Light trace arrows mark the residues and connectivities from ligand-kringle Overhauser experiments depicted in figures 5, 7, 8. Irradiated residues are shown circled; arrows are directed away from the irradiated side chain and point to neighbor groups in close contact. Arrows denoting strong or fast build-up NOEs are marked by continuous (—) trace while for those showing weak or slow build-up NOEs, likely to originate *via* spin-diffusion, a dashed (– – –) trace is used.

chain(s) at the binding site. This interpretation is supported by the shifts experienced by BASA (figure 5) and by the Overhauser experiments described above. In particular, the efficient cross-relaxation between BASA and the shifted Trp-II triplet and Trp-III singlet unambiguously demonstrate that two indole groups are in direct contact with the ligand ring. Indeed, tryptophans must be very important for the structure of the five human plasminogen kringles, since they are consistently found at sites 25 and 62. Residue 72 is Trp in kringles 2, 3, and 4, and Tyr, another aromatic amino acid, in kringles 1 and 5 (Sottrup-Jensen *et al.,* 1978). Thus, the aromatic rings that show cross-relaxation with BASA are likely to contribute to the large shifts of the bound-ligand resonances while affording lipophilic components that help retain the ligand at the

binding site. A model that we have favoured is of a hydrophobic channel or groove with Asp^{57} in the interior of the protein and Arg^{71} near the surface, the two charged groups being at a distance of ~ 6·8 Å from each other to optimally pair complementary electrostatic charges on the ligand-dipole.

Our model for the ligand-kringle interaction highlights the role of the Cys^{51}–Cys^{75} loop (figure 1) in structuring the lysine-binding site (Trexler and Patthy, 1983; De Marco *et al.,* 1985a) and suggests that Trp-II might correspond to Trp^{62} and, by exclusion, Trp-I to Trp^{25}. The assignment of Trp-II to Trp^{62} would be consistent with the observation that Trp-II exhibits a characteristic pH titration profile in both kringle 1 (to be published) and K4 (De Marco *et al.,* 1985b) reflecting proximity of the indole ring to a free carboxylic acid group: within the Cys^{51} – Cys^{75} loop, sites 55, 57 and 67 are filled by Asp residues in the two kringles and site 73 is occupied by Asp in kringle 1 and Glu in K4. On the basis of selective phenol ring nitration, Trexler *et al.* (1983) have assigned Tyr-II to Tyr^{50} and Tyr-III to Tyr^{41}, and suggested that Tyr-IV might correspond to Tyr^{74}. The latter assignment receives further circumstantial support from the Overhauser experiments described here. We have observed that irradiation of Trp-II H2 singlet perturbs strongly Tyr-IV regardless of whether BASA is present or not (figure 6A′, B′). Furthermore, irradiation of Leu^{46}, centered at the kringle's hydrophobic core, does not indicate cross-relaxation with Tyr-IV which, in turn, happens to be perturbed upon irradiation of Trp^{72} (Trp-III) at the lysine-binding site. This suggests that Tyr-IV is located closer to (or within) the loop defining the binding site than it is to the hydrophobic core, contiguous to the site (figure 1). Since Tyr-II has been assigned to Tyr^{50}, Tyr^{74} remains as the other Tyr residue closest to the loop so that it can be tentatively assigned to Tyr-IV. His-I is likely to be His^{3} (Trexler *et al.,* 1983) and, since His-II is His^{31} (Llinás *et al.,* 1983), it follows that His-III is likely to be His^{33}. Added insights are contributed by the effect of εACA on the six lysyl CH_2^{ε} resonances of K4 (figure 10), Upon ligand additions two CH_2^{ε} multiplets shift (figure 10B, C), while the other four exhibit only the characteristic, generalized sharpening brought about by ligand-binding. It is highly unlikely that Lys^{20} and Lys^{21} (figure 1) interact with εACA because the disruption of the Cys^{1} –Cys^{80} disulphide bridge does not influence the ligand-binding ability of K4 (Trexler and Patthy, 1983, 1984). Similarly, Lys^{78} and Lys^{79} are adjacent to Cys^{80} (figure 1) and would probably become less structured on cleavage of the Cys^{1} – Cys^{80} bond. More likely to experience interactions with the ligand are Lys^{58}, proximal to Asp^{57}, and Lys^{35}, which has been reported to be close to Trp^{72} (Trexler *et al.,* 1983).

Trexler and Patthy (1983) have shown that Cys^{22}–Cys^{63} and Cys^{51}–Cys^{75} bridges, the latter one defining the lysine-binding loop, are the first to form during the folding of K4, suggesting that they are essential for maintaining the native conformation. Such a proposal is in agreement with our preliminary scheme for kringle folding (De Marco *et al.*, 1985a) which requires that the region stretching between sites 30 and 50, namely most of the Cys^{22}–Cys^{63} loop, be folded toward the Cys^{51}–Cys^{75} loop, contributing to the hydrophobic core which adjoins the lysine-binding site. It is suggested that BASA and Leu^{46} are separated by aromatic residues that stabilize ligand-binding and fix the structure of the hydrophobic core. In fact, we know that one of the Leu^{46} methyl groups is adjacent to Tyr-III (Tyr^{41}) while the other interacts with both Trp-I and Trp-II (Llinás *et al.,* 1983; Trexler *et al*., 1983; De Marco *et al*., 1985a) so that a model

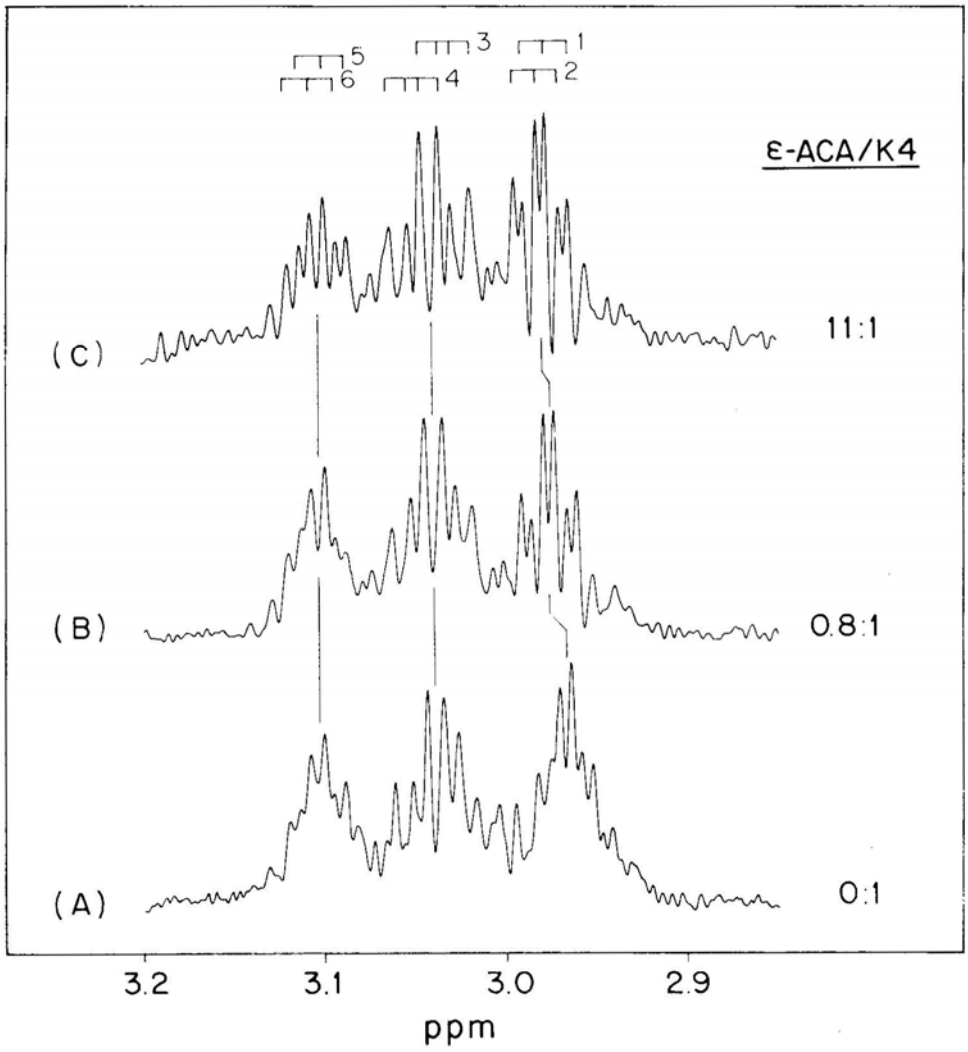

Figure 10. Effect of εACA-binding on lysyl $CH_{\varepsilon 2}$ proton resonances of K4 at 600 MHz. The $CH_{\varepsilon 2}$ multiplets from the six lysyl residues are indicated in spectrum C. Vertical lines between spectra connect corresponding groups of resonances; breaks denote shifts induced by ligand-binding. K4 concentration was ~ 10^{-3} *M*; pH* 7·2, 25°C. All spectra are resolution-enhanced.

suggests itself by which Leu46 would be adjacent to the Trp-II indole which, in turn, would separate it from the binding site. While more structural information is required in order to further substantiate and improve this primitive model, our studies definitively point to the primary role played by aromatic residues in defining the K4 ligand-binding site and the constellation of side chains that surrounds it.

Acknowledgements

This research was supported by the US Public Health Service, National Institutes of Health Grants HL–15535 and HL–29409. The 600 MHz NMR facility is supported by the US Public Health Service, National Institutes of Health Grant RR–00292.

Note added in proof

Recent 2-D NMR experiments on ligand-binding by K4 have shown that the resonance shift identified as Tyr-V in figures 4 and 5 does in fact arise from Phe^{64} (Ramesh, V., Laursen, R. A. and Llinás, M., unpublished results). While this observation adds support to the Overhauser experiments (figure 7) in demonstrating a close interaction between the site 64 residue and the ligand, it removes evidence for a direct participation of the structurally constrained Tyr-V side chain in ligand-binding.

References

Bothner-by, A. A. (1979) in *Biological Applications of Magnetic Resonance,* (ed. R. G. Shulman) (New York; Academic Press) p. 177.
Bovey, F. A. (1969) *Nuclear Magnetic Resonance Spectroscopy,* (New York: Academic Press) p. 264.
De Marco, A. (1977) *J. Magn. Reson.*, **26,** 527.
De Marco, A., Hochschwender, S. M., Laursen, R. A., and Llinás, M. (1982) *J. Biol. Chem.*, **257,** 12716.
De Marco, A., Laursen, R. A., and Llinás, M. (1985a) *Biochim. Biophys. Acta,* 827, 369.
De Marco, A., Pluck, N. D., Bányai. L., Trexler, M., Laursen, R. A. Patthy, L., Llinás. M. and Williams, R. J. P. (1985b) *Biochemistry*, **24,** 748.
De Marco, A., Motta, A., Laursen, R. A. and Llinás, M. (1985c) *Biophys. J.,* (in press).
Ernst, R. E. (1966) *Adv. Magn. Reson.,* **2,** 1.
Ferrige, A. G. and Lindon, J. C. (1978) *J. Magn. Reson.,* **31,** 337.
Hochschwender, S. M. and Laursen, R. A. (1981) *J. Biol. Chem.,* **256,** 11172.
Hochschwender, S. M., Laursen. R. A. De Marco, A. and Llinás, M. (1983) *Arch. Biochem. Biophys.,* **223,** 58.
Lerch. P. G. and Rickli, E. E. (1980) *Biochim. Biophys. Acta*. **625,** 374.
Lerch, P. G., Rickli. E. E., Lergier. W. and Gillessen. D. (1980) *Eur. J. Biochem*., **107,** 7.
Llinás, M., De Marco, A., Hochschwender, S. M. and Laursen, R. A. (1983) *Eur. J. Biochem.,* **135,** 379.
Mark wardt, F. (1978) in Fibrinolytics and Antifibrinolytics (ed. F. Markward,) (Berlin: Springer-Verlag) p. 511.
Okamoto, S., Oshiba, S., Mihara, H. and Okamoto, U. (1968) *Ann. N. Y. Acad. Sci.,* **146,** 414.
Patthy, L., Trexler, M., Váli, Z., Bányai, L. and Varadi, A. (1984) *FEBS Lett.,* **171,** 131.
Perkins, S. J. (1982) *Biol. Magn. Resonance,* **4,** 193.
Sottrup-Jensen, L., Claeys, H., Zajdel, M., Petersen, T. E. and Magnusson, S. (1978) *Progr. Chem. Fibrinolysis Trombolysis,* **3,** 191.
Trexler, M., Váli, Z. and Patthy, L. (1982) *J. Biol. Chem.,* **257,** 7401.
Trexler, M., Bányai, L., Patthy, L., Pluck, N. D. and Williams, R. J. P. (1983) *FEBS Lett.,* **154,** 311.
Trexler, M. and Patthy, L. (1983) *Proc. Natl. Acad. Sci. USA*, **80,** 2457.
Trexler, M. and Patthy, L. (1984) *Biochim. Biophys. Acta,* **787,** 275.
Winn, E. S., Hu, S. P., Hochschwender, S. M. and Laursen. R. A. (1980) *Eur. J. Biochem.,* **104,** 579.